Environmental Science & Technology Letters

pubs.acs.org/journal/estlcu

Letter

Aquifer-Scale Observations of Iron Redox Transformations in Arsenic-Impacted Environments to Predict Future Contamination

Athena A. Nghiem,* Yating Shen, Mason Stahl, Jing Sun, Ezazul Haque, Beck DeYoung, Khue N. Nguyen, Tran Thi Mai, Pham Thi Kim Trang, Hung Viet Pham, Brian Mailloux, Charles F. Harvey, Alexander van Geen, and Benjamin C. Bostick*

Cite This: *Environ. Sci. Technol. Lett.* 2020, 7, 916−922

Read Online

ACCESS | Metrics & More | Article Recommendations | Supporting Information

ABSTRACT: Iron oxides control the mobility of a host of contaminants in aquifer systems, and the microbial reduction of iron oxides in the subsurface is linked to high levels of arsenic in groundwater that affects greater than 150 million people globally. Paired observations of groundwater and solid-phase aquifer composition are critical to understand spatial and temporal trends in contamination and effectively manage changing water resources, yet field-representative mineralogical data are sparse across redox gradients relevant to arsenic contamination. We characterize iron mineralogy using X-ray absorption spectroscopy across a natural gradient of groundwater arsenic contamination in Vietnam. Hierarchical cluster analysis classifies sediments into meaningful groups delineating weathering and redox changes, diagnostic of depositional history, in this first direct characterization of redox transformations in the field. Notably, these groupings reveal a signature of iron minerals undergoing active reduction before the onset of arsenic contamination in groundwater. Pleistocene sediments undergoing postdepositional reduction may be more extensive than previously recognized due to previous misclassification. By upscaling to similar environments in South and Southeast Asia via multinomial logistic regression modeling, we show that active iron reduction, and therefore susceptibility to future arsenic contamination, is more widely distributed in presumably pristine aquifers than anticipated.

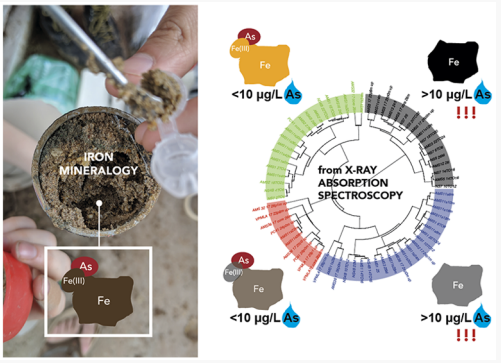

INTRODUCTION

Groundwater contaminated by arsenic exposes more than 150 million people globally to toxic levels above the World Health Organization (WHO) limit of 10 μg/L.[1,2] Arsenic is a systemic toxin that leads to major adverse health outcomes.[3,4] To reduce exposure to high arsenic, people across South and Southeast Asia increasingly rely on older Pleistocene aquifers as a safer alternative to younger Holocene aquifers that commonly have high concentrations of arsenic in groundwater.[5] Alarmingly, recent evidence shows that the typically pristine Pleistocene aquifers are susceptible to reduction and arsenic contamination.[6−10] Arsenic release into groundwater is commonly attributed to microbially mediated reductive dissolution of arsenic-bearing iron (Fe) (oxyhydr)oxide minerals in the subsurface.[11,12] Measurements of aqueous groundwater arsenic are extensive, but comparably few studies examine iron minerals or their postdeposition stability and transformations in arsenic-impacted environmental settings. Although solid phases have been previously characterized, most have been part of laboratory-based experiments or are sampled too sparsely to identify relevant chemical gradients in detail.[13−16] Consequently, we do not fully understand the extent of geochemical transformations that occur as sediments undergo reduction and impact groundwater arsenic concentrations in the field, particularly where Pleistocene aquifers could be the locus of future contamination.

The limited observations available to distinguish iron mineralogy or sediment age are based on proxies using sediment color or chemical compositions that differ between sediment lithology or ages.[6,17] One of the few measurements, especially of redox state, is color of aquifer sands from field observations and spectral reflectance measurements.[18] Color is often used as an indicator of safer wells because Pleistocene-aged sediments often appear orange-colored and contain presumably more oxidized Fe minerals, while Holocene sediments appear gray and contain presumably more reduced Fe minerals, leading to their differences in dissolved arsenic concentrations.[1,6,19] However, color itself does not uniquely identify depositional history or transformations due to active redox processes (e.g., Pleistocene sediment that has been reduced and turned gray) or presence of other minerals or

Received: August 21, 2020
Revised: September 28, 2020
Accepted: September 28, 2020
Published: September 30, 2020

https://dx.doi.org/10.1021/acs.estlett.0c00672
Environ. Sci. Technol. Lett. 2020, 7, 916−922

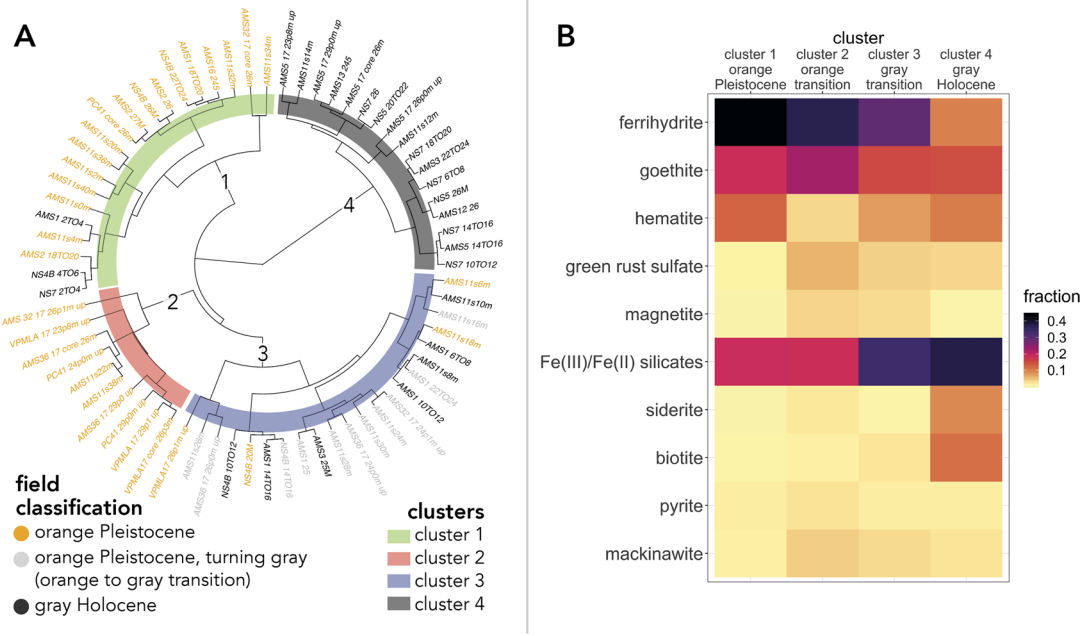

Figure 1. (A) Dendrogram shows clusters identified by hierarchical cluster analysis match with and expand on field classification of sediment redox state and depositional history. The clusters that naturally arise from the branching of the dendrogram are labeled by highlighted color (cluster 1 in green, cluster 2 in red, cluster 3 in blue, cluster 4 in black); the cluster number is also denoted on each branch of the dendrogram. Each sample name on the dendrogram includes the well name and sediment depth and is colored by field-identified classifications, where an orange sample name represents orange Pleistocene sediment, a gray sample name represents orange Pleistocene sediment that is turning gray (known as part of the "orange to gray" transition zone), and a black sample name represents gray Holocene sediment per field classification. (B) Heat map shows higher fraction of oxidized Fe(III) minerals in more oxidized clusters and higher fraction of reduced Fe(II) minerals in clusters undergoing reduction. From top to bottom on the *y*-axis, Fe minerals are listed from more oxidized Fe(III) minerals (ferrihydrite, goethite, hematite) to mixed Fe(III)/Fe(II) minerals (green rust, magnetite, mixed Fe(III)/Fe(II) silicates) to more reduced Fe(II) minerals (siderite, a secondary Fe(II) carbonate; biotite, a primary Fe(II) silicate; pyrite; mackinawite). From left to right, the clusters are listed from more oxidized (orange Pleistocene) to more reduced (gray Holocene). The gradient from yellow (lower fraction) to purple (higher fraction) indicates the mean fraction of Fe mineral of each cluster from linear combination fitting.

organic matter. X-ray absorption spectroscopy (XAS) is uniquely suited to analyze redox state and mineralogy in sediments across geologic transitions.[20] Recent developments in XAS have greatly increased sample throughput to enable collection of relatively large data sets of sediment mineralogy across environmental gradients.[21] Using this approach, we classify sediments into groups of similar depositional history and redox state based on their iron speciation and mineralogy to provide a comprehensive view of Fe reduction processes.

Here, we analyze XAS spectra of 134 core samples from 24 sediment cores drilled in transitional environments in the Red River Delta near Hanoi, Vietnam in the villages of Van Phuc, Van Duc, and Yen My (Figure S1). In Van Phuc, a sharp gradient laterally separates a Pleistocene aquifer, with groundwater arsenic concentrations lower than the WHO limit, from a Holocene aquifer with arsenic concentrations 10 to 30 times the WHO limit.[6] At this boundary, the Pleistocene aquifer is becoming contaminated and creating a transition zone of arsenic release.[6,22,23] This large XAS data set differentiates the mineralogy of oxidized orange Pleistocene and gray reduced Holocene settings from environments undergoing postdepositional reductive change. We investigate evidence of active weathering and redox processes determined by Fe mineralogy to relate mineralogical changes to changes in aqueous composition and arsenic across a redox gradient. Then, we leverage this relationship to predict the distribution of transitional sediments (i.e., undergoing active reduction) that could be at risk of contamination in similar deltaic settings across South and Southeast Asia.

MATERIALS AND METHODS

Study Area and Sampling. The study area is located south of Hanoi, Vietnam, in the Red River Delta. Sediment cores were drilled in Van Phuc, Van Duc, and Yen My[6,7,23] (Figure S1) by either push or piston coring (details in SI). From the core sections, subsamples of approximately every meter were collected, mixed 1:1 with glycerol immediately in the field, and stored in microcentrifuge tubes at −20 °C until analysis to best preserve the redox state as previously reported.[24,25] No indication of oxidation occurred (SI). Aqueous chemistry and sediment field characterizations were previously reported and characterized for these sites;[6,23,26] radiocarbon dating of select cores was performed at the National Ocean Sciences Accelerator Mass Spectrometry facility, as previously reported[10] (SI).

X-ray Absorption Spectroscopy. Glycerol-preserved sediment samples were analyzed via XAS at Stanford Synchrotron Radiation Lightsource on beamlines 4-1 and 11-2 and Argonne National Laboratory Advanced Photon Source on beamline 10-BM. Fe extended X-ray absorption fine structure (EXAFS) spectra of prepped samples were collected under beamline conditions as previously reported[25,27,28] (SI).

Statistical Analysis. Normalization of Fe EXAFS spectra was done in SIXPACK.[29] Principal components analysis was performed with SIXPACK on all Fe EXAFS samples and 10 Fe

https://dx.doi.org/10.1021/acs.estlett.0c00672
Environ. Sci. Technol. Lett. 2020, 7, 916−922

standards. Linear combination fitting was performed using k^3-weighted chi functions with a k range from 1 to 12 (with package "penalized" in R) and restricted to non-negative fits. The principal component (PC) loadings were exported from SIXPACK for hierarchical cluster analysis performed in the statistical program R. Hierarchical clustering analysis was performed on PC1 to PC4 based on Euclidean distance using Ward's minimum variance method from which a dendrogram shows the splitting of different clusters (see details in SI).

A supervised multinomial logistic regression model was developed to predict the defined sediment classifications based on the concentrations of aqueous arsenic, manganese, and iron that distinguish between redox zones in Van Phuc. The model was trained with a 70%/30% split training/test set; cross-validation was performed in R (SI). To upscale to South and Southeast Asia, the model was run on a data set of aqueous concentrations that we compiled from previously published studies (USGS Powell Center Database, Table S1, n = 10675). The compiled data set of aqueous iron, manganese, and arsenic were used to predict the sediment mineralogy for each available sample.

RESULTS AND DISCUSSION

Spectroscopic Differentiation of Redox Gradient. Direct characterizations of iron mineralogy across geochemical gradients are necessary to accurately identify specific mineralogical changes associated with increasing groundwater arsenic. The principal component loadings of Fe EXAFS spectra correlate to sediment color, redox state, and weathering (Text S2, Figure S3, Data S1). Sediment groupings classified by hierarchical cluster analysis of principal components effectively differentiates gray Holocene sediments from the orange Pleistocene and transition zone sediments (Figure 1A). The first branching point in the dendrogram separates gray Holocene sediments from others, which are presumed Pleistocene,[6] but span a wide range of presumed redox states based on color. Cluster 4 is tentatively assigned to represent these gray Holocene sediments. The second and third branching point differentiates the other sediments into three groups. The second branch defines cluster 1, which represents orange, oxidized Pleistocene sediments based on field classification. A tertiary node separates clusters 2 and 3. Cluster 2 is similar to other orange Pleistocene sediments; cluster 3 contains the field-identified transition zone sediments.

Previous observations of this redox transition in Van Phuc have focused on the color and position of cored sediments across the sharp transition between the orange Pleistocene and gray Holocene aquifers.[6] Many of our XAS measurements are adjacent to this transition zone to better characterize subtle Fe reduction more widely. Cluster 3 contains sediments that were seemingly misclassified based on color in field observations as orange Pleistocene sediment or gray Holocene sediments (Figure 1). The mineralogical similarity in these misclassified sediments suggest that they are transitional. In cluster 3, the initially field-identified *orange* sediments were actually in the process of conversion to gray or toward the boundary close to orange−gray transition. Moreover, in cluster 3, the initially field-identified *gray* sediments (and thus presumed Holocene) are actually converted Pleistocene sediments that appeared gray and reduced, suggesting that the transition zone is more extensive than previously expected (Figure S4). It is important to note that our classification is based on mineralogical transformations resulting from redox changes and weathering and not strictly age; however, this work suggests Pleistocene sediments may be misclassified by more traditional approaches as gray Holocene sediments, once they have undergone extensive reduction.[6,18] The extent of the transition zone as either permanently or transitionally reduced affects our understanding of arsenic release mechanisms and water quality.

Finally, while cluster 2 visually appears orange based on field classification and reflectance measurements, its mineralogy clusters closely to that of transition zone sediments (cluster 3) (Figure 1A). This suggests that sediments in cluster 2 also are transitional but that the transition has not been sufficient to change their appearance. The successively decreasing iron oxidation state and the extent of reduction in each cluster is observed in the Fe K-edge positions of their X-ray absorption near-edge structure spectra (Figure S5). Hierarchical cluster analysis identifies four groups that are particularly useful to understand active redox transformations of iron oxides in field environments and their effect on dissolved arsenic levels: Cluster 1 represents orange Pleistocene, and clusters 2 and 3 are more oxidized (orange transition) and more reduced (gray transition) transitional Pleistocene environments, respectively, while cluster 4 is separately gray Holocene. Radiocarbon dating confirms these classifications using redox processes as an indirect proxy for depositional and postdepositional history (Table S2). These classifications are equally applicable when we expand our classifications to nearby villages (SI).

Classifying sediments into groups greatly improves contextualization of underlying mineralogies quantified for each sample via conventional linear combination fitting (Figure S2). When the linear combination fits of samples are considered cohesively in clusters as opposed to individually, as is typically done, sediment groups show clear differences in the relative abundance of primary and secondary Fe minerals indicative of their weathering history and redox status (Figure 1B, Figure S6). Orange Pleistocene sediments are mostly composed of reactive Fe(III) oxyhydroxides such as ferrihydrite (and nanogoethite) and oxidized Fe(III) minerals, like goethite and hematite, but low mean fraction of reduced Fe minerals other than primary silicates[25] (Figure 1B, Figure S6). Comparatively, the gray Holocene cluster is composed of a lower mean fraction of reactive ferrihydrite but a high fraction of secondary mineral and reactive Fe(II) carbonate, siderite. Siderite is significantly ($p < 0.05$) higher in the gray Holocene cluster than in the other Pleistocene clusters. This agrees well with the assumption that gray Holocene sediments are generally more reduced and form siderite from dissolved Fe(II).[30,31] The mean fraction of biotite, a primary Fe(II) silicate mineral, is also higher for the gray Holocene sediments than the mean fraction of biotite in all other Pleistocene clusters. Differences in the abundance fraction of primary minerals between Holocene and Pleistocene sediments may reflect variations in the source or type of sediment transported and deposited in the Holocene and Pleistocene due to geological and climatic changes affecting river sediment. More likely, Holocene sediments contain more biotite because they are younger and subjected to less extensive chemical weathering,[32] consistent with findings of detrital biotite associated with Holocene sediments.[33]

The transitions observed as sediments undergo reduction from the orange Pleistocene to the orange transition to the gray transition cluster provide the first direct characterization of the redox transformations in a field environment affected by arsenic. Reduction is evident from the decrease in the mean

https://dx.doi.org/10.1021/acs.estlett.0c00672
Environ. Sci. Technol. Lett. 2020, 7, 916−922

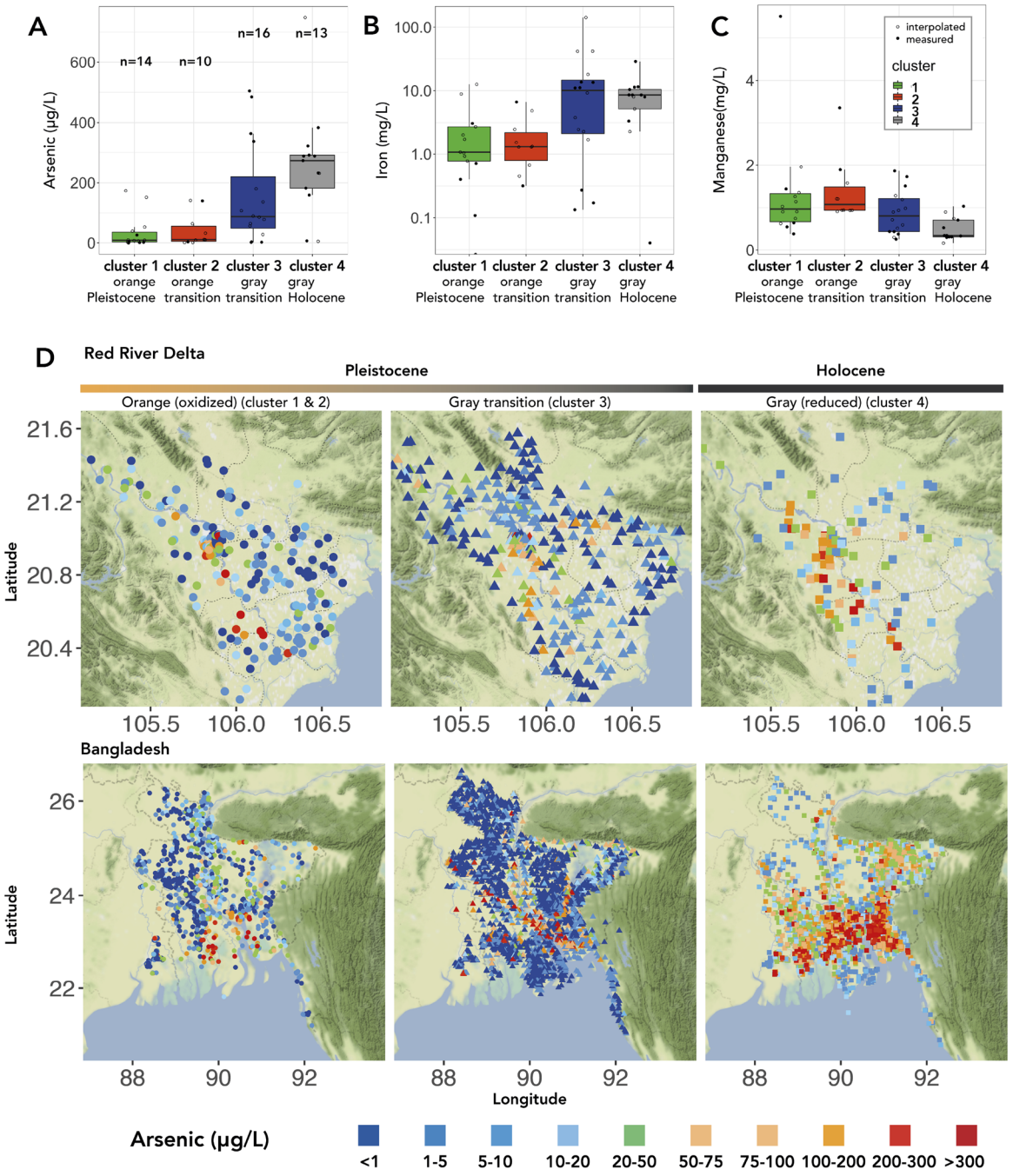

Figure 2. Aqueous (A) arsenic, (B) iron, and (C) manganese from the field site are used to train a supervised classification model to classify sediment redox and depositional age by clusters (D). Boxplot of measured and interpolated aqueous (A) arsenic, (B) iron, and (C) manganese concentrations as grouped by sediment clusters in Van Phuc. (D) Map of classified sediment distribution results in Red River Delta, Vietnam, and Bangladesh by cluster as colored by aqueous arsenic concentrations. Note that clusters 1 and 2 are grouped together as orange sediments in the classification model, and clusters 1, 2, and 3 represent Pleistocene sediments. Base map is from Google Maps imagery.[47]

fraction of ferrihydrite and in the tail of the goethite histogram (where poorly crystalline goethite is reduced), leading to release of arsenic (Figure S6).[30] Mineral transformations also produce higher mixed Fe(III)/Fe(II) silicate abundance in both clusters of gray sediments (clusters 3 and 4) that are arsenic-contaminated zones. Here, mixed Fe(III)/(II) silicates are representative of a wide variety of secondary clays and the primary mineral hornblende, which share a similar Fe octahedral coordination structure.[34] Secondary clays may create the visually gray sediment appearance identified in the field from the reduction of more oxidized Fe minerals. Moreover, green rust found in the transition zone is produced in soils but is seldom quantified as it is reactive and usually is either oxidized or converted to more stable Fe(II) minerals such as magnetite or siderite.[35,36] Green rust can form as the secondary Fe mineral product following ferrihydrite dissolution (at higher arsenic concentrations) as well as during the conversion from ferrihydrite to magnetite.[37,38] Importantly, green rust can exclude arsenic[37] and could contribute to increased arsenic release into groundwater in the transition zone. Notably, we are able to quantify the extent of supposed redox transformations in the field environment that are not as

https://dx.doi.org/10.1021/acs.estlett.0c00672
Environ. Sci. Technol. Lett. 2020, 7, 916−922

readily apparent from sediment Fe concentrations alone (Figure S7).

Linking Sediment Classification and Aqueous Compositions. Solution composition and groundwater arsenic levels can change rapidly in response to modest changes in sediment mineralogy and redox state.[39] We probe this relationship by linking paired sediment cluster groupings and aqueous composition directly related to arsenic release. As generally expected in oxidized environments with abundant Fe(III) oxides, the orange Pleistocene group (cluster 1) has generally low aqueous arsenic and Fe concentrations (Figure 2A,B). Interestingly, although there is evidence of reduction in the Fe mineralogy, aqueous arsenic remains low in the orange transition zone (cluster 2); this suggests that dissolved arsenic concentration does not increase until there is extensive iron reduction, at least for Pleistocene sediments (Figure 2A). The more reduced gray transition zone sediments (cluster 3) have variable but often much higher aqueous arsenic and Fe concentrations than the orange transition zone sediments (cluster 2). Wells within these zones (clusters 1−3) contain varied evidence of Fe reduction forming metastable Fe(II) minerals but consistently high aqueous Mn (Figure 2C). The orange transition zone (cluster 2) has the highest aqueous Mn concentrations but low sediment Mn concentrations, suggesting reduction of Mn oxides can act as a buffer before more extensive Fe reduction[40] (Figure S7). The aqueous arsenic and Fe concentrations in the gray transition zone (cluster 3) are comparable to those of gray Holocene sediments (cluster 4), where reduction is prevalent. The conversion and corresponding increase in groundwater arsenic can be quite rapid in perturbed systems. In Van Phuc, this conversion has occurred over 50−60 years due to the reversal in groundwater flow from pumping in Hanoi.[6] The cross section of the transect (Figure S4) suggests a clear evolution of mineralogy during sediment reduction that influences aqueous composition. Because this reduction occurs due to groundwater flow,[6] orange transitional environments are likely also indicators of groundwater plumes and preferential flow along the redox boundary.[41] These orange transition zones form at the front of a migrating groundwater plume and serve as lenses for more extensive sediment reduction and future increases in groundwater arsenic.

The mineralogical analysis shows a clear relationship between sediment redox transformations revealed by detailed Fe mineralogy and groundwater composition. In particular, the potential contamination of pristine aquifers as distinguished by the mineralogical signature is critical to identify before evidence of arsenic contamination is found in the aqueous data. Given that the aqueous composition of different sediment groups is distinct, the local observation is directly scalable to similar deltaic aquifers in South and Southeast Asia based on measurements of groundwater composition that are more widely available.

The multinomial logistic regression model of iron mineralogy successfully differentiates sediments into their mineralogical clusters in Van Phuc (Table S3), based on the aqueous predictors of iron, arsenic, and manganese. The model is readily translated to predict Fe redox processes within the similar sediments of deltaic environments across South and Southeast Asia, where extensive mineralogical data may not yet exist but where extensive aqueous concentrations have been measured (Data S3). In the Red River Delta, there is a patchwork of Pleistocene and Holocene sediments, and many Pleistocene sediments appear to be undergoing redox transformations,[8] similar to in Cambodia with suggested Mn reduction buffering Fe reduction.[40] In the Ganges−Brahmaputra−Meghna Delta in Bangladesh, this method faithfully predicts major geological features of Pleistocene terraces and Holocene paleo-alluvial valleys[17,42−45] (Figure S9). Other aqueous species that vary sharply across redox transition zones but were not used as predictors, including phosphate, ammonium, and sulfate, clearly corroborate redox transformations and weathering delineated by mineralogical classifications (Figure S10). This exercise suggests that approximately 49% of aquifers recorded in the compiled database are transitional aquifers in South and Southeast Asia, which could be susceptible to future arsenic contamination (Data S3).

This overall method provides a general framework for relating mineralogy to aqueous composition that can be readily extended to understand biogeochemical processes occurring in other environments; it is directly applicable to understanding arsenic in glacial aquifers, where extended synchrotron data has been reported.[46] Our results suggest that previously identified high-arsenic deltaic aquifers widely believed to be gray Holocene are actually Pleistocene aquifers that have undergone extensive reduction; this implies aquifers currently supplying low arsenic groundwater may not necessarily continue to do so in the future. The distribution of transitional versus permanently reduced environments also questions our fundamental understanding of whether associated reduction has increased over time due to more recent hydrological changes such as extensive anthropogenic pumping or has always continuously existed in a state of transition.

■ ASSOCIATED CONTENT

Supporting Information

The Supporting Information is available free of charge at https://pubs.acs.org/doi/10.1021/acs.estlett.0c00672.

Text, figures, tables, and data files (PDF)
Correlations and fits (XLSX)
Core data (XLSX)
Specific data clusters (ZIP)

■ AUTHOR INFORMATION

Corresponding Authors

Benjamin C. Bostick − *Lamont-Doherty Earth Observatory, Columbia University, Palisades, New York 10964, United States;* orcid.org/0000-0002-7513-6469; Phone: +1 845 365 8659; Email: bostick@ldeo.columbia.edu; Fax: +1 845 365 8155

Athena A. Nghiem − *Department of Earth and Environmental Sciences and Lamont-Doherty Earth Observatory, Columbia University, New York, New York 10027, United States;* orcid.org/0000-0001-9135-0804; Phone: +1 845 365 8572; Email: anghiem@ldeo.columbia.edu; Fax: +1 845 365 8155

Authors

Yating Shen − *Lamont-Doherty Earth Observatory, Columbia University, Palisades, New York 10964, United States; National Research Center of Geoanalysis, Chinese Academy of Geological Sciences, Beijing, China*

Mason Stahl − *Department of Geology, Union College, Schenectady, New York 12308, United States*

https://dx.doi.org/10.1021/acs.estlett.0c00672
Environ. Sci. Technol. Lett. 2020, 7, 916−922

Jing Sun − *State Key Laboratory of Environmental Geochemistry, Institute of Geochemistry, Chinese Academy of Sciences, Guiyang, China;* orcid.org/0000-0002-0129-5184
Ezazul Haque − *Department of Occupational and Environmental Health, University of Iowa, Iowa City, Iowa 52242, United States*
Beck DeYoung − *Department of Geology, Union College, Schenectady, New York 12308, United States*
Khue N. Nguyen − *Lamont-Doherty Earth Observatory, Columbia University, Palisades, New York 10964, United States*
Tran Thi Mai − *Key Laboratory of Analytical Technology for Environmental Quality and Food Safety Control (KLATEFOS), VNU University of Science, Vietnam National University, Hanoi, Vietnam*
Pham Thi Kim Trang − *Key Laboratory of Analytical Technology for Environmental Quality and Food Safety Control (KLATEFOS), VNU University of Science, Vietnam National University, Hanoi, Vietnam*
Hung Viet Pham − *Key Laboratory of Analytical Technology for Environmental Quality and Food Safety Control (KLATEFOS), VNU University of Science, Vietnam National University, Hanoi, Vietnam;* orcid.org/0000-0002-9016-0694
Brian Mailloux − *Department of Environmental Sciences, Barnard College, New York, New York 10027, United States*
Charles F. Harvey − *Department of Civil and Environmental Engineering, Massachusetts Institute of Technology, Cambridge, Massachusetts 02139, United States*
Alexander van Geen − *Lamont-Doherty Earth Observatory, Columbia University, Palisades, New York 10964, United States;* orcid.org/0000-0003-2073-9841

Complete contact information is available at: https://pubs.acs.org/10.1021/acs.estlett.0c00672

Notes

The authors declare no competing financial interest.

■ ACKNOWLEDGMENTS

This work was supported by National Science Foundation (NSF) Grant EAR 15-21356, National Institute of Environmental Health Sciences Grant ES010349, Partnerships for Enhanced Engagement in Research (PEER) Project 2-544, and an NSF Graduate Research Fellowship to A.A.N. The authors gratefully thank Carl Johnson and Timothy Eglinton for the radiocarbon data measured at the National Ocean Sciences Accelerator Mass Spectrometry (NOSAMS) facility. This research used resources of the Advanced Photon Source, a U.S. Department of Energy (DOE) Office of Science User Facility operated for the DOE Office of Science by Argonne National Laboratory under Contract No. DE-AC02-06CH11357. Use of the Stanford Synchrotron Radiation Lightsource, SLAC National Accelerator Laboratory, is supported by the U.S. Department of Energy, Office of Science, Office of Basic Energy Sciences under Contract No. DE-AC02-76SF00515. The database and part of this work was conducted as a part of the Characterizing Global Variability in Groundwater Arsenic Working Group supported by the John Wesley Powell Center for Analysis and Synthesis, funded by the U.S. Geological Survey. Data from this working group is openly accessible at Columbia Academic Commons (https://doi.org/10.7916/d8-zenj-yx36). This is LDEO Contribution number 8447.

■ REFERENCES

(1) Fendorf, S.; Michael, H. A.; van Geen, A. Spatial and Temporal Variations of Groundwater Arsenic in South and Southeast Asia. *Science (Washington, DC, U. S.)* **2010**, *328* (5982), 1123−1127.
(2) Podgorski, J.; Berg, M. Global Threat of Arsenic in Groundwater. *Science (Washington, DC, U. S.)* **2020**, *368* (6493), 845−850.
(3) Wasserman, G. A.; Liu, X.; Parvez, F.; Ahsan, H.; Factor-Litvak, P.; van Geen, A.; Slavkovich, V.; Lolacono, N. J.; Cheng, Z.; Hussain, I.; Momotaj, H.; Graziano, J. H. Water Arsenic Exposure and Children's Intellectual Function in Araihazar, Bangladesh. *Environ. Health Perspect.* **2004**, *112* (13), 1329−1333.
(4) Quansah, R.; Armah, F. A.; Essumang, D. K.; Luginaah, I.; Clarke, E.; Marfoh, K.; Cobbina, S. J.; Nketiah-Amponsah, E.; Namujju, P. B.; Obiri, S.; Dzodzomenyo, M. Association of Arsenic with Adverse Pregnancy Outcomes/Infant Mortality. *Environ. Health Perspect.* **2015**, *123* (5), 412−421.
(5) Michael, H. A.; Voss, C. I. Evaluation of the Sustainability of Deep Groundwater as an Arsenic-Safe Resource in the Bengal Basin. *Proc. Natl. Acad. Sci. U. S. A.* **2008**, *105* (25), 8531−8536.
(6) van Geen, A.; Bostick, B. C.; Thi Kim Trang, P.; Lan, V. M.; Mai, N.-N.; Manh, P. D.; Viet, P. H.; Radloff, K.; Aziz, Z.; Mey, J. L.; Stahl, M. O.; Harvey, C. F.; Oates, P.; Weinman, B.; Stengel, C.; Frei, F.; Kipfer, R.; Berg, M. Retardation of Arsenic Transport through a Pleistocene Aquifer. *Nature* **2013**, *501* (7466), 204−207.
(7) Berg, M.; Trang, P. T. K.; Stengel, C.; Buschmann, J.; Viet, P. H.; Van Dan, N.; Giger, W.; Stuben, D. Hydrological and Sedimentary Controls Leading to Arsenic Contamination of Groundwater in the Hanoi Area, Vietnam: The Impact of Iron-Arsenic Ratios, Peat, River Bank Deposits, and Excessive Groundwater Abstraction. *Chem. Geol.* **2008**, *249* (1−2), 91−112.
(8) Winkel, L. H. E.; Trang, P. T. K.; Lan, V. M.; Stengel, C.; Amini, M.; Ha, N. T.; Viet, P. H.; Berg, M. Arsenic Pollution of Groundwater in Vietnam Exacerbated by Deep Aquifer Exploitation for More than a Century. *Proc. Natl. Acad. Sci. U. S. A.* **2011**, *108* (4), 1246−1251.
(9) Mozumder, M. R. H.; Michael, H. A.; Mihajlov, I.; Khan, M. R.; Knappett, P. S. K.; Bostick, B. C.; Mailloux, B. J.; Ahmed, K. M.; Choudhury, I.; Koffman, T.; Ellis, T.; Whaley-Martin, K.; San Pedro, R.; Slater, G.; Stute, M.; Schlosser, P.; Geen, A. Origin of Groundwater Arsenic in a Rural Pleistocene Aquifer in Bangladesh Depressurized by Distal Municipal Pumping. *Water Resour. Res.* **2020**, *56* (7), 1−26.
(10) Mihajlov, I.; Mozumder, M. R. H.; Bostick, B. C.; Stute, M.; Mailloux, B. J.; Knappett, P. S. K.; Choudhury, I.; Ahmed, K. M.; Schlosser, P.; van Geen, A. Arsenic Contamination of Bangladesh Aquifers Exacerbated by Clay Layers. *Nat. Commun.* **2020**, *11* (1), na DOI: 10.1038/s41467-020-16104-z.
(11) Nickson, R. T.; Mcarthur, J. M.; Ravenscroft, P.; Burgess, W. G.; Ahmed, K. M. Mechanism of Arsenic Release to Groundwater, Bangladesh and West Bengal. *Appl. Geochem.* **2000**, *15* (4), 403−413.
(12) Harvey, C. F.; Swartz, C. H.; Badruzzaman, A. B. M.; Keon-Blute, N.; Yu, W.; Ali, M. A.; Jay, J.; Beckie, R.; Niedan, V.; Brabander, D.; Oates, P. M.; Ashfaque, K. N.; Islam, S.; Hemond, H. F.; Ahmed, M. F. Arsenic Mobility and Groundwater Extraction in Bangladesh. *Science (Washington, DC, U. S.)* **2002**, *298* (5598), 1602−1606.
(13) Quicksall, A. N.; Bostick, B. C.; Sampson, M. L. Linking Organic Matter Deposition and Iron Mineral Transformations to Groundwater Arsenic Levels in the Mekong Delta, Cambodia. *Appl. Geochem.* **2008**, *23* (11), 3088−3098.
(14) Polizzotto, M. L.; Harvey, C. F.; Sutton, S. R.; Fendorf, S. Processes Conducive to the Release and Transport of Arsenic into Aquifers of Bangladesh. *Proc. Natl. Acad. Sci. U. S. A.* **2005**, *102* (52), 18819−18823.
(15) Polizzotto, M. L.; Harvey, C. F.; Li, G.; Badruzzman, B.; Ali, A.; Newville, M.; Sutton, S.; Fendorf, S. Solid-Phases and Desorption Processes of Arsenic within Bangladesh Sediments. *Chem. Geol.* **2006**, *228* (1−3), 97−111.
(16) Postma, D.; Jessen, S.; Hue, N. T. M.; Duc, M. T.; Koch, C. B.; Viet, P. H.; Nhan, P. Q.; Larsen, F. Mobilization of Arsenic and Iron

from Red River Floodplain Sediments, Vietnam. *Geochim. Cosmochim. Acta* **2010**, *74* (12), 3367−3381.
(17) Goodbred, S. L.; Paolo, P. M.; Ullah, M. S.; Pate, R. D.; Khan, S. R.; Kuehl, S. A.; Singh, S. K.; Rahaman, W. Piecing Together the Ganges-Brahmaputra-Meghna River Delta: Use of Sediment Provenance to Reconstruct the History and Interaction of Multiple Fluvial Systems during Holocene Delta Evolution. *Geol. Soc. Am. Bull.* **2014**, *126* (11−12), 1495−1510.
(18) Horneman, A.; van Geen, A.; Kent, D. V.; Mathe, P. E.; Zheng, Y.; Dhar, R. K.; O'Connell, S.; Hoque, M. A.; Aziz, Z.; Shamsudduha, M.; Seddique, A. A.; Ahmed, K. M. Decoupling of As and Fe Release to Bangladesh Groundwater under Reducing Conditions. Part I: Evidence from Sediment Profiles. *Geochim. Cosmochim. Acta* **2004**, *68* (17), 3459−3473.
(19) Hossain, M.; Bhattacharya, P.; Frape, S. K.; Jacks, G.; Islam, M. M.; Rahman, M. M.; von Brömssen, M.; Hasan, M. A.; Ahmed, K. M. Sediment Color Tool for Targeting Arsenic-Safe Aquifers for the Installation of Shallow Drinking Water Tubewells. *Sci. Total Environ.* **2014**, *493*, 615−625.
(20) Shoenfelt, E. M.; Winckler, G.; Annett, A. L.; Hendry, K. R.; Bostick, B. C. Physical Weathering Intensity Controls Bioavailable Primary Iron(II) Silicate Content in Major Global Dust Sources. *Geophys. Res. Lett.* **2019**, *46* (19), 10854−10864.
(21) Lombi, E.; Susini, J. Synchrotron-Based Techniques for Plant and Soil Science: Opportunities, Challenges and Future Perspectives. *Plant Soil* **2009**, *320* (1−2), 1−35.
(22) Neidhardt, H.; Winkel, L. H. E.; Kaegi, R.; Stengel, C.; Trang, P. T. K.; Lan, V. M.; Viet, P. H.; Berg, M. Insights into Arsenic Retention Dynamics of Pleistocene Aquifer Sediments by in Situ Sorption Experiments. *Water Res.* **2018**, *129*, 123−132.
(23) Stahl, M. O.; Harvey, C. F.; van Geen, A.; Sun, J.; Thi Kim Trang, P.; Mai Lan, V.; Mai Phuong, T.; Hung Viet, P.; Bostick, B. C. River Bank Geomorphology Controls Groundwater Arsenic Concentrations in Aquifers Adjacent to the Red River, Hanoi Vietnam. *Water Resour. Res.* **2016**, *52*. 863216334.
(24) Gnanaprakasam, E. T.; Lloyd, J. R.; Boothman, C.; Ahmed, K. M.; Choudhury, I.; Bostick, B. C.; van Geen, A.; Mailloux, B. J. Microbial Community Structure and Arsenic Biogeochemistry in Two Arsenic-Impacted Aquifers in Bangladesh. *mBio* **2017**, *8* (6), 1−18.
(25) Sun, J.; Mailloux, B. J.; Chillrud, S. N.; van Geen, A.; Thompson, A.; Bostick, B. C. Simultaneously Quantifying Ferrihydrite and Goethite in Natural Sediments Using the Method of Standard Additions with X-Ray Absorption Spectroscopy. *Chem. Geol.* **2018**, *476*, 248−259.
(26) Nghiem, A. A.; Stahl, M. O.; Mailloux, B. J.; Mai, T. T.; Trang, P. T.; Viet, P. H.; Harvey, C. F.; Geen, A.; Bostick, B. C. Quantifying Riverine Recharge Impacts on Redox Conditions and Arsenic Release in Groundwater Aquifers Along the Red River, Vietnam. *Water Resour. Res.* **2019**, *55* (8), 6712−6728.
(27) Shoenfelt, E. M.; Sun, J.; Winckler, G.; Kaplan, M. R.; Borunda, A. L.; Farrell, K. R.; Moreno, P. I.; Gaiero, D. M.; Recasens, C.; Sambrotto, R. N.; Bostick, B. C. High Particulate iron(II) Content in Glacially Sourced Dusts Enhances Productivity of a Model Diatom. *Sci. Adv.* **2017**, *3* (6), e1700314.
(28) Shoenfelt, E. M.; Winckler, G.; Lamy, F.; Anderson, R. F.; Bostick, B. C. Highly Bioavailable Dust-Borne Iron Delivered to the Southern Ocean during Glacial Periods. *Proc. Natl. Acad. Sci. U. S. A.* **2018**, *115* (44), 11180.
(29) Webb, S. M. SIXPack a Graphical User Interface for XAS Analysis Using IFEFFIT. *Phys. Scr.* **2005**, *1011*, 1011.
(30) Sø, H. U.; Postma, D.; Vi, M. L.; Pham, T. K. T.; Kazmierczak, J.; Dao, V. N.; Pi, K.; Koch, C. B.; Pham, H. V.; Jakobsen, R. Arsenic in Holocene Aquifers of the Red River Floodplain, Vietnam: Effects of Sediment-Water Interactions, Sediment Burial Age and Groundwater Residence Time. *Geochim. Cosmochim. Acta* **2018**, *225*, 192−209.
(31) Eiche, E.; Neumann, T.; Berg, M.; Weinman, B.; van Geen, A.; Norra, S.; Berner, Z.; Trang, P. T. K.; Viet, P. H.; Stüben, D. Geochemical Processes Underlying a Sharp Contrast in Groundwater Arsenic Concentrations in a Village on the Red River Delta, Vietnam. *Appl. Geochem.* **2008**, *23* (11), 3143−3154.
(32) Mailloux, B. J.; Alexandrova, E.; Keimowitz, A. R.; Wovkulich, K.; Freyer, G. A.; Herron, M.; Stolz, J. F.; Kenna, T. C.; Pichler, T.; Polizzotto, M. L.; Dong, H.; Bishop, M.; Knappett, P. S. K. Microbial Mineral Weathering for Nutrient Acquisition Releases Arsenic. *Appl. Environ. Microbiol.* **2009**, *75* (8), 2558−2565.
(33) Ravenscroft, P.; Burgess, W. G.; Ahmed, K. M.; Burren, M.; Perrin, J. Arsenic in Groundwater of the Bengal Basin, Bangladesh: Distribution, Field Relations, and Hydrogeological Setting. *Hydrogeol. J.* **2005**, *13* (5−6), 727−751.
(34) Hawthorne, F. C.; Oberti, R.; Harlow, G. E.; Maresch, W. V.; Martin, R. F.; Schumacher, J. C.; Welch, M. D. Nomenclature of the Amphibole Supergroup. *Am. Mineral.* **2012**, *97* (11−12), 2031−2048.
(35) Schwertmann, U.; Taylor, R. M. Iron Oxides. In *Minerals in Soil Environments*; Soil Science Society of America, 1989; Chapter 8, pp 379−438. DOI: 10.2136/sssabookser1.2ed.c8.
(36) Cornell, R. M.; Schwertmann, U. The Iron Oxides: Structure, Properties, Reactions, Occurrences and Uses. *Techniques* **2003**, *39* (8), 9−12.
(37) Kocar, B. D.; Borch, T.; Fendorf, S. Arsenic Repartitioning during Biogenic Sulfidization and Transformation of Ferrihydrite. *Geochim. Cosmochim. Acta* **2010**, *74* (3), 980−994.
(38) Sumoondur, A.; Shaw, S.; Ahmed, I.; Benning, L. G. Green Rust as a Precursor for Magnetite: An *in situ* Synchrotron Based Study. *Mineral. Mag.* **2008**, *72* (1), 201−204.
(39) Buschmann, J.; Berg, M. Impact of Sulfate Reduction on the Scale of Arsenic Contamination in Groundwater of the Mekong, Bengal and Red River Deltas. *Appl. Geochem.* **2009**, *24* (7), 1278−1286.
(40) Gillispie, E. C.; Matteson, A. R.; Duckworth, O. W.; Neumann, R. B.; Phen, N.; Polizzotto, M. L. Chemical Variability of Sediment and Groundwater in a Pleistocene Aquifer of Cambodia: Implications for Arsenic Pollution Potential. *Geochim. Cosmochim. Acta* **2019**, *245*, 441−458.
(41) Wallis, I.; Prommer, H.; Berg, M.; Siade, A. J.; Sun, J.; Kipfer, R. The River−groundwater Interface as a Hotspot for Arsenic Release. *Nat. Geosci.* **2020**, *13* (April), 288.
(42) Zheng, Y.; Stute, M.; Van Geen, A.; Gavrieli, I.; Dhar, R.; Simpson, H. J.; Schlosser, P.; Ahmed, K. M. Redox Control of Arsenic Mobilization in Bangladesh Groundwater. *Appl. Geochem.* **2004**, *19* (2), 201−214.
(43) Goodbred, S. L.; Kuehl, S. A.; Steckler, M. S.; Sarker, M. H. Controls on Facies Distribution and Stratigraphic Preservation in the Ganges-Brahmaputra Delta Sequence. *Sediment. Geol.* **2003**, *155* (3−4), 301−316.
(44) Acharyya, S. K.; Lahiri, S.; Raymahashay, B. C.; Bhowmik, A. Arsenic Toxicity of Groundwater in Parts of the Bengal Basin in India and Bangladesh: The Role of Quaternary Stratigraphy and Holocene Sea-Level Fluctuation. *Environ. Geol.* **2000**, *39* (10), 1127−1137.
(45) Morgan, J. P.; McIntire, W. G. Quaternary Geology of the Bengal Basin, East Pakistan and India. *Geol. Soc. Am. Bull.* **1959**, *70* (3), 319−342.
(46) Nicholas, S. L.; Erickson, M. L.; Woodruff, L. G.; Knaeble, A. R.; Marcus, M. A.; Lynch, J. K.; Toner, B. M. Solid-Phase Arsenic Speciation in Aquifer Sediments: A Micro-X-Ray Absorption Spectroscopy Approach for Quantifying Trace-Level Speciation. *Geochim. Cosmochim. Acta* **2017**, *211*, 228−255.
(47) Kahle, D.; Wickham, H. Ggmap : Spatial Visualization with. *R J.* **2013**, *5* (1), 144−161.

https://dx.doi.org/10.1021/acs.estlett.0c00672
Environ. Sci. Technol. Lett. 2020, 7, 916−922